Available online at www.sciencedirect.com
ScienceDirect
Journal of Sound and Vibration 317 (2008) 236–249
JOURNAL OF SOUND AND VIBRATION
www.elsevier.com/locate/jsvi

# Symplectic analysis of vertical random vibration for coupled vehicle–track systems

F. Lu[a,b], D. Kennedy[b], F.W. Williams[b], J.H. Lin[a,*]

[a]*State Key Laboratory of Structural Analysis of Industrial Equipment, Dalian University of Technology, Dalian 116023, People's Republic of China*
[b]*Cardiff School of Engineering, Cardiff University, Cardiff CF24 3AA, UK*

Received 22 August 2006; received in revised form 25 February 2008; accepted 2 March 2008
Handling Editor: L.G. Tham

**Abstract**

A computational model for random vibration analysis of vehicle–track systems is proposed and solutions use the pseudo excitation method (PEM) and the symplectic method. The vehicle is modelled as a mass, spring and damping system with 10 degrees of freedom (dofs) which consist of vertical and pitching motion for the vehicle body and its two bogies and vertical motion for the four wheelsets. The track is treated as an infinite Bernoulli–Euler beam connected to sleepers and hence to ballast and is regarded as a periodic structure. Linear springs couple the vehicle and the track. Hence, the coupled vehicle–track system has only 26 dofs. A fixed excitation model is used, i.e. the vehicle does not move along the track but instead the track irregularity profile moves backwards at the vehicle velocity. This irregularity is assumed to be a stationary random process. Random vibration theory is used to obtain the response power spectral densities (PSDs), by using PEM to transform this random multiexcitation problem into a deterministic harmonic excitation one and then applying symplectic solution methodology. Numerical results for an example include verification of the proposed method by comparing with finite element method (FEM) results; comparison between the present model and the traditional rigid track model and; discussion of the influences of track damping and vehicle velocity.


## 1. Introduction

Track irregularity is well known to be an important source of vibration of coupled vehicle–track systems, where the track consists of a pair of rails supported by sleepers and ballast. Therefore, it is necessary to study the random vibration characteristics of such systems. The present paper is restricted to vertical vibrations, i.e. rotation of the vehicle about its longitudinal and vertical axes are ignored.

Two kinds of excitation model are available for analyzing this coupled system, namely fixed excitation and moving excitation ones. In the fixed excitation model, it is assumed that the vehicle is stationary while the track irregularity moves backwards at the vehicle velocity. This model can account for both vibration of the vehicle and wheel–rail contact forces and it enables solutions to be obtained relatively easily in the frequency

*Corresponding author. Tel.: +86 411 84709403; fax: +86 411 84708400.
*E-mail address:* jhlin@dlut.edu.cn (J.H. Lin).

0022-460X/$ - see front matter © 2008 Elsevier Ltd. All rights reserved.
doi:10.1016/j.jsv.2008.03.004

domain. In the moving excitation model, the vehicle moves along the track at its actual velocity $V$, which is more realistic. However, the system is time dependent and so is much harder to analyze by random vibration theory.

Only a few studies have concentrated on random vibration analysis of vehicle–track systems. Chen [1] derived response power spectral densities (PSDs) by using the fixed excitation model and random vibration theory. Nonlinear contact springs have also been used to account for elasticity of the wheels and rails adjacent to their contact points [2,3]. The first step in this approach [2,3] is to calculate the dynamic responses in the time domain by using a sample of the track profile irregularity derived from its PSD, and then transforming these responses into the frequency domain to get response PSDs. As yet, there is no mature random vibration theory for such nonlinear problems. Therefore, the objective of the present paper is to study this problem by using the fixed excitation model and the linear random vibration theory and to show that this gives a very efficient method.

Two difficulties arise during computational analysis of the random vibration of the coupled system. The first difficulty is that the number of degrees of freedom (dofs) is very large, e.g. 400–500 dof are necessary for the vertical model [1,4]. The second difficulty is that the problem is a multiexcitation one, for which the excitations at the interaction points between the wheelset and the rails are correlated, so that the random vibration analysis is very time consuming. The first difficulty can be overcome by regarding the track as a periodic structure [5–8]. In recent years a new solution method has been proposed for wave propagation in periodic structures, which employs symplectic methodology [9–12] and has been used to investigate random wave propagation [13–15]. The second difficulty has been overcome by using the fact that there are only time lags between the excitations in order to transform the multiexcitation problem into a generalized single excitation one [1,16–18].

The present paper uses a computational model of the vehicle–track system to perform random vibration analysis by combining the pseudo excitation method (PEM) and a symplectic solution method. This combination is very powerful because it has been shown [16–18] that PEM is easily the fastest way to deal with random multiexcitation problems, which it transforms into deterministic harmonic excitations, regardless of whether the excitations are fully or only partially coherent. The vehicle is modelled as its body, two bogies and four wheelsets, which are connected by spring and damping systems. Hence, the model has 10 dofs, consisting of vertical and pitching motion of the vehicle body and bogies and; vertical motion of the wheelsets (see Fig. 1, which is described in more detail later). The rails are treated as an infinite Euler beam elastically connected to sleepers and hence to ballast to form the longitudinally periodic track. Linear springs are used to couple the vehicle and track to represent local elasticity, as described above. The resulting coupled system has only 26 dofs. In this paper, a fixed excitation method is used, i.e. instead of the vehicle moving forwards with velocity $V$, the track irregularity moves backwards at velocity $V$ and is taken to be a stationary random process.

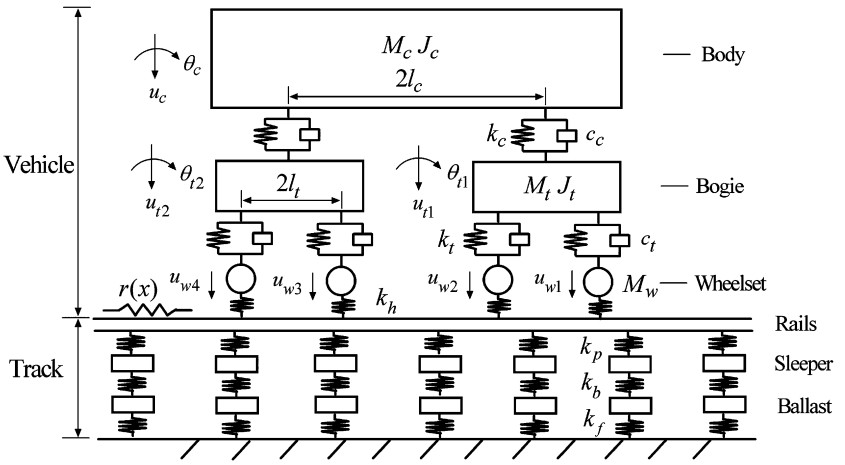


Fig. 1. Model of vehicle–track coupled system. Here $M$ (or $m$), $k$, $c$ and $J$ denote, respectively, for each of the components shown, mass, stiffness, damping coefficient and rotatory moment of inertia.

The response PSD is derived from random vibration theory by using PEM to transform the random multiexcitation problem into a deterministic harmonic excitation problem for which symplectic solution methodology is applied to solve the harmonic responses of the vehicle and track systems. A numerical example is used to verify the proposed method and its associated computer program by comparing results with those given by finite element method (FEM). Then comparison between the present model and the traditional rigid track model is made and the influence of track damping and vehicle velocity is discussed. Finally, some useful conclusions are drawn.

## 2. The fixed model for the vehicle–track system

The model used for random vibration analysis of the vehicle–track system is shown in Fig. 1. The vehicle body and its bogies are treated as rigid and the vehicle is modelled by these and by the two layers of springs and dampers shown, so that there are 10 dofs, consisting of vertical and rotational (about the transverse axis) motion of the vehicle body ($u_c$, $\theta_c$) and its two identical bogies ($u_{t1}$, $\theta_{t1}$, $u_{t2}$ and $\theta_{t2}$), plus the vertical motion of the four rigid wheelsets ($u_{w1}$, $u_{w2}$, $u_{w3}$ and $u_{w4}$). The track consists of a pair of rails, which are modelled as a single infinite beam, and sleepers and ballast, which support it via the springs shown. $r(x)$ is the track irregularity, which varies with distance $x$ and can be taken as a stationary random process. The irregularity moves backwards at the vehicle velocity $V$. In general, the springs used to represent the local elasticity of the wheels and rails at their contact points are nonlinear ones, which are based on the Hertz formula, but in the random vibration theory of this paper the linearized spring [1]

$$k_h = 3P_0^{1/3}/G$$

is assumed, where $P_0$ is the static wheel–rail load between one wheel and one rail, $G$ is the contact constant and the spring $k_h$ represents contact between a wheelset and the pair of rails. Hence, the entire system of Fig. 1 is linear and independent of time.

## 3. PEM for stationary fully correlated multiexcitation

PEM can deal with stationary or nonstationary multiexcitation problems, which are either fully or partially correlated, but only stationary and fully correlated multiexcitation is covered by this paper, as follows. Note that this section gives the key equations only, because their derivation has been given elsewhere [17,18].

Consider a structure with $n$ dofs and subjected to $m$ stationary out-of-phase excitations. Its equation of motion is

$$\mathbf{M}\ddot{\mathbf{y}} + \mathbf{C}\dot{\mathbf{y}} + \mathbf{K}\mathbf{y} = \mathbf{J}\mathbf{f}(t) \tag{1}$$

where $t$ is the time, $\mathbf{y}$ is the displacement vector; $\mathbf{M}$, $\mathbf{C}$ and $\mathbf{K}$ are the mass, damping and stiffness matrices, respectively; $\mathbf{J}$ is an $n \times m$ constant matrix which expresses the excitation distribution within the structure and; $\mathbf{f}(t)$ is a random excitation vector in which each element is derived from the same excitation source $F(t)$ via Eq. (2):

$$\mathbf{f}(t) = \{a_1F(t-t_1), \quad a_2F(t-t_2), \quad \cdots \quad a_mF(t-t_m)\}^{\mathrm{T}} \tag{2}$$

Here, $t_j$ ($j = 1, 2, \ldots, m$) is the time lag; $a_j$ is a constant coefficient which expresses the intensity of the excitation and; the superscript T denotes transpose.

If $S_{FF}(\omega)$ is defined as the PSD of $F(t)$, where $\omega$ is the frequency, then the input PSD matrix $\mathbf{S}_{\mathrm{in}}(\omega)$ of the excitation can be expressed as

$$\mathbf{S}_{\mathrm{in}}(\omega) = \begin{bmatrix} a_1^2 & a_1a_2\,\mathrm{e}^{\mathrm{i}\omega(t_1-t_2)} & \cdots & a_1a_m\,\mathrm{e}^{\mathrm{i}\omega(t_1-t_m)} \\ a_2a_1\,\mathrm{e}^{\mathrm{i}\omega(t_2-t_1)} & a_2^2 & \cdots & a_2a_m\,\mathrm{e}^{\mathrm{i}\omega(t_2-t_m)} \\ \cdots & \cdots & \cdots & \cdots \\ a_ma_1\,\mathrm{e}^{\mathrm{i}\omega(t_m-t_1)} & a_ma_2\mathrm{e}^{\mathrm{i}\omega(t_m-t_2)} & \cdots & a_m^2 \end{bmatrix} S_{FF}(\omega) \tag{3}$$

Then random vibration theory enables the response PSD matrix $\mathbf{S}_{\text{out}}(\omega)$ to be written as

$$\mathbf{S}_{\text{out}}(\omega) = \mathbf{H}^*(\omega)\mathbf{S}_{\text{in}}(\omega)\mathbf{H}(\omega)^{\text{T}} \tag{4}$$

in which $\mathbf{H}(\omega)$ is the frequency-response matrix and the asterisk denotes complex conjugate and the superscript T denotes transpose.

It would be very time consuming to compute the matrix $\mathbf{S}_{\text{out}}(\omega)$ directly from Eq. (4) and so PEM is used instead, as follows. Assume that the structure is subjected to a pseudo excitation

$$\tilde{\mathbf{f}}(t) = \{a_1\,\mathrm{e}^{-\mathrm{i}\omega\,t_1} \quad a_2\mathrm{e}^{-\mathrm{i}\omega\,t_2} \quad \ldots \quad a_m\mathrm{e}^{-\mathrm{i}\omega\,t_m}\}\sqrt{S_{FF}(\omega)}\,\mathrm{e}^{\mathrm{i}\omega t} \tag{5}$$

Then, the corresponding response vector will be $\tilde{\mathbf{y}} = \mathbf{H}(\omega)\tilde{\mathbf{f}}(t)$. It has been proved in Ref. [17] that a vector $\tilde{\mathbf{y}}$ can be found such that multiplying its complex conjugate by its transpose gives $\mathbf{S}_{\text{out}}(\omega)$, i.e.

$$\mathbf{S}_{\text{out}} = \tilde{\mathbf{y}}^*\tilde{\mathbf{y}}^{\text{T}} \tag{6}$$

Hence, the velocity and acceleration response PSD's matrix, $S_v$ and $S_a$, can be obtained as, respectively,

$$\mathbf{S}_v = \omega^2\mathbf{S}_{\text{out}}, \quad \mathbf{S}_a = \omega^4\mathbf{S}_{\text{out}} \tag{7}$$

Note that PEM transforms random multiexcitation into harmonic excitation and avoids matrix multiplication.

In the present paper, the excitation source $F(t)$ becomes the track irregularity $r(x)$ and so the excitation vector $\mathbf{f}(t)$ becomes $\mathbf{R}(x)$, where

$$\mathbf{R}(x) = \{r(x), r(x-2l_t), r(x-2l_c), r(x-2l_t-2l_c)\}^{\text{T}} \tag{8}$$

Note that here the intensity of excitation at each wheel–rail contact point is the same and equal to 1, i.e. $a_j = 1$, and instead of times lags there are now only distance lags between the elements of $\mathbf{R}(x)$. Therefore, because the vehicle is treated as stationary, so that the irregularity moves backwards with velocity $V$, we have $x = Vt$ (note that this implies that the $x$ axis is horizontal and points to the left on Fig. 1). Substituting this into Eq. (8) and using PEM, the pseudo excitation vector can be constituted as

$$\tilde{\mathbf{R}}(t) = \{r_1, r_2, r_3, r_4\}^{\text{T}} = \{\mathrm{e}^{-\mathrm{i}\omega t_1}, \mathrm{e}^{-\mathrm{i}\omega t_2}, \mathrm{e}^{-\mathrm{i}\omega t_3}, \mathrm{e}^{-\mathrm{i}\omega t_4}\}^{\text{T}}\sqrt{\tilde{S}_r(\omega)}\,\mathrm{e}^{\mathrm{i}\omega t} \tag{9}$$

$$t_1 = 0, \quad t_2 = 2l_t/V, \quad t_3 = 2l_c/V, \quad t_4 = 2(l_t + l_c)/V, \quad \tilde{S}_r(\omega) = S_r(\Omega)/V, \quad \Omega = \omega/V$$

Note that it is assumed that $S_r(\Omega)$, the PSD of $r(x)$, is known and that Eq. (9) means that the coupled system has a deterministic harmonic irregularity for each $\Omega$ as its input, so that the corresponding responses are now considered.

## 4. Symplectic analysis of track frequency-response characteristics

Section 4.1 gives the key aspects of the well-established [9–12] symplectic solution method for solving wave propagation problems for periodic structures and then Section 4.2 shows how it is applied to the track.

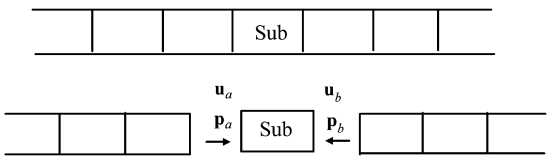


Fig. 2. A periodic structure.

### 4.1. Wave propagation in periodic structures

Fig. 2 shows a periodic structure in which a harmonic wave with frequency $\omega$ is assumed to propagate. The undamped equations of motion of the substructure can be partitioned to give

$$(\mathbf{K}-\omega^2\mathbf{M})\begin{Bmatrix}\mathbf{u}_i\\ \mathbf{u}_a\\ \mathbf{u}_b\end{Bmatrix}=\begin{bmatrix}\mathbf{K}^0_{ii} & \mathbf{K}^0_{ia} & \mathbf{K}^0_{ib}\\ \mathbf{K}^0_{ai} & \mathbf{K}^0_{aa} & \mathbf{K}^0_{ab}\\ \mathbf{K}^0_{bi} & \mathbf{K}^0_{ba} & \mathbf{K}^0_{bb}\end{bmatrix}\begin{Bmatrix}\mathbf{u}_i\\ \mathbf{u}_a\\ \mathbf{u}_b\end{Bmatrix}=\begin{Bmatrix}\mathbf{p}_i\\ \mathbf{p}_a\\ \mathbf{p}_b\end{Bmatrix} \tag{10}$$

where $\mathbf{u}_a$ and $\mathbf{u}_b$ are the displacement vectors at the left- and right-hand interfaces; $\mathbf{u}_i$ is an internal displacement vector and; $\mathbf{p}_a$, $\mathbf{p}_b$ and $\mathbf{p}_i$ are the corresponding nodal force vectors. Now $\mathbf{u}_a$, $\mathbf{u}_b$, $\mathbf{p}_a$, $\mathbf{p}_b$ and $\mathbf{p}_i$ can be expressed in mode space as

$$\mathbf{u}_a=\mathbf{X}_b\mathbf{b},\quad \mathbf{u}_b=\mathbf{X}_a\mathbf{a} \tag{11a}$$

$$\mathbf{p}_a=\mathbf{p}_{ae}-\mathbf{P}_b\mathbf{u}_a,\quad \mathbf{p}_b=\mathbf{p}_{be}-\mathbf{P}_a\mathbf{u}_b,\quad \mathbf{p}_i=\mathbf{p}_{ie} \tag{11b}$$

$$\mathbf{P}_a=\mathbf{N}_a\mathbf{X}_a^{-1},\quad \mathbf{P}_b=-\mathbf{N}_b\mathbf{X}_b^{-1}$$

where $\mathbf{a}$ and $\mathbf{b}$ are coefficient vectors; $\mathbf{p}_{ae}$, $\mathbf{p}_{be}$ and $\mathbf{p}_{ie}$ are external harmonic load vectors; $\mathbf{P}_a$ and $\mathbf{P}_b$ are the dynamic stiffness matrices at the two interfaces of the substructure, respectively; and $\mathbf{X}_a$, $\mathbf{X}_b$, $\mathbf{N}_a$ and $\mathbf{N}_b$ are square matrices which are obtained from the eigenvectors of the wave propagation transformation matrix $\mathbf{S}(\omega)$, see Eq. (13), as follows:

$$\mathbf{S}(\omega)=\begin{bmatrix}\mathbf{S}_{aa} & \mathbf{S}_{ab}\\ \mathbf{S}_{ba} & \mathbf{S}_{bb}\end{bmatrix} \tag{12}$$

$$\mathbf{S}_{aa}=-\mathbf{K}_{ab}^{-1}\mathbf{K}_{aa},\quad \mathbf{S}_{ab}=\mathbf{K}_{ab}^{-1}$$
$$\mathbf{S}_{ba}=-\mathbf{K}_{ba}+\mathbf{K}_{bb}\mathbf{K}_{ab}^{-1}\mathbf{K}_{aa},\quad \mathbf{S}_{bb}=-\mathbf{K}_{bb}\mathbf{K}_{ab}^{-1}$$

$$\mathbf{K}_{aa}=\mathbf{K}^0_{aa}-\mathbf{K}^0_{ai}(\mathbf{K}^0_{ii})^{-1}\mathbf{K}^0_{ia},\quad \mathbf{K}_{ab}=\mathbf{K}^0_{ab}-\mathbf{K}^0_{ai}(\mathbf{K}^0_{ii})^{-1}\mathbf{K}^0_{ib}$$
$$\mathbf{K}_{bb}=\mathbf{K}^0_{bb}-\mathbf{K}^0_{bi}(\mathbf{K}^0_{ii})^{-1}\mathbf{K}^0_{ib},\quad \mathbf{K}_{ba}=\mathbf{K}^{\mathrm{T}}_{ab}$$

It has been proved in Ref. [12] that $\mathbf{S}(\omega)$ is a symplectic matrix and that if $\mu$ is an eigenvalue of $\mathbf{S}(\omega)$, then so is $1/\mu$. These eigenvalues are called propagation coefficients because they express the wave propagation characteristics. Now assume that $\mathbf{S}(\omega)$ has $2n$ eigenvalues and let them be separated into two groups:

$$(a)\ \mu_i\quad i=1,2,\ldots,n;\quad |\mu_i|\leqslant 1,\quad (b)\quad \mu_{n+i}=1/\mu_i,\quad i=1,2,\ldots,n,\quad |\mu_{n+i}|\geqslant 1$$

Hence, the corresponding eigenvectors can be used to constitute the matrix

$$\mathbf{\Phi}=\begin{bmatrix}\boldsymbol{\varphi}_1, & \boldsymbol{\varphi}_2, & \ldots, & \boldsymbol{\varphi}_{2n}\end{bmatrix}\equiv\begin{bmatrix}\mathbf{X}_a & \mathbf{X}_b\\ \mathbf{N}_a & \mathbf{N}_b\end{bmatrix} \tag{13}$$

For a loaded substructure, substituting Eq. (11) into Eq. (10) gives

$$\begin{bmatrix}\mathbf{K}^*_{aa} & \mathbf{K}^*_{ab}\\ \mathbf{K}^*_{ba} & \mathbf{K}^*_{bb}\end{bmatrix}\begin{Bmatrix}\mathbf{b}\\ \mathbf{a}\end{Bmatrix}=\begin{Bmatrix}\mathbf{p}^*_a\\ \mathbf{p}^*_b\end{Bmatrix} \tag{14}$$

$$\mathbf{K}^*_{aa}=(\mathbf{K}_{aa}+\mathbf{P}_b)\mathbf{K}_b,\quad \mathbf{K}^*_{ab}=\mathbf{K}_{ab}\mathbf{X}_a$$

$$\mathbf{K}^*_{bb}=(\mathbf{K}_{bb}+\mathbf{P}_a)\mathbf{K}_a,\quad \mathbf{K}^*_{ba}=\mathbf{K}_{ba}\mathbf{X}_b$$

$$\mathbf{p}^*_a=\mathbf{p}_{ae}-\mathbf{K}^0_{ai}(\mathbf{K}^0_{ii})^{-1}\mathbf{p}_{ie},\quad \mathbf{p}^*_b=\mathbf{p}_{be}-\mathbf{K}^0_{bi}(\mathbf{K}^0_{ii})^{-1}\mathbf{p}_{ie}$$

Eq. (14) is the wave propagation equation of a loaded substructure for which $\mathbf{p}_{ae}$, $\mathbf{p}_{be}$ and $\mathbf{p}_{ie}$ represents the load. If an external harmonic load acts on any chosen substructure, it will generate two waves, which propagate, respectively, to its left and to its right. If $\mathbf{a}$ and $\mathbf{b}$ of the substructure are obtained by solving Eq. (14), it is possible to obtain any required response at the $k$th interface, where positive $k$ is to the right of the loaded substructure and negative $k$ is to its left, with the zeroth interface being between the loaded substructure and the one to its right for $k>0$ and to its left for $k<0$:

$$\mathbf{u}_{kr} = \mathbf{X}_a \boldsymbol{\mu}^k \mathbf{a}, \quad \mathbf{p}_{kr} = \mathbf{P}_a \mathbf{u}_{kr}, \quad k \geqslant 0 \tag{15a}$$

$$\mathbf{u}_{kl} = \mathbf{X}_b \boldsymbol{\mu}^{-k} \mathbf{b}, \quad \mathbf{p}_{kl} = -\mathbf{P}_b \mathbf{u}_{kl}, \quad k \leqslant 0 \tag{15b}$$

Here, $\boldsymbol{\mu}$ is a diagonal matrix of order $n$, in which the $i$th diagonal element is $\mu_i$ ($|\mu_i| \leqslant 1$), i.e. $\boldsymbol{\mu}$ consists of the $\mu_i$ of (a), see Eq. (13).

Damping is neglected in the above derivation, but hysteretic damping can be included simply by multiplying the above static stiffness matrices by $e^{iv}$ [13–15], where $i = \sqrt{-1}$ and $v$ is a damping coefficient ($0 < v \ll 1$). Thus, Eq. (10) can be rewritten as

$$(\mathbf{K} - \beta \mathbf{M}) \begin{Bmatrix} \mathbf{u}_i \\ \mathbf{u}_a \\ \mathbf{u}_b \end{Bmatrix} = e^{-iv} \begin{Bmatrix} \mathbf{p}_i \\ \mathbf{p}_a \\ \mathbf{p}_b \end{Bmatrix}, \quad \beta = e^{-iv} \omega^2 \tag{16}$$

Comparison between Eqs. (16) and (10) shows that all the above derivations are still valid if $\omega^2$ is replaced by $\beta$ and the nodal force vectors are multiplied by $e^{iv}$.

### 4.2. Model of the track

The track is regarded as a periodic structure in which the substructure consists of the pair of rails between neighboring sleepers, a sleeper and the associated ballast, see Fig. 3. For this substructure, the mass of the sleeper and ballast are $m_s$ and $m_b$, respectively, and the pair of rails is represented by a single Bernoulli–Euler beam of length $l$, flexural rigidity $EI$ and mass per unit length $m_r$. Additionally, the elastic properties of the rail pad, ballast and subgrade are represented by the equivalent springs with the stiffnesses shown on Fig. 3, i.e. $k_p$, $k_b$ and $k_f$, respectively. The substructure has 6 dofs, i.e. 2 dofs of the beam representing the rails at each of its two interfaces and 2 dofs of the sleeper and ballast. Therefore, there will be two propagation coefficients of which the absolute value is no greater than 1. The static stiffness matrix $\mathbf{K}$ and the mass matrix $\mathbf{M}$ of a substructure needed by Eq. (10) are

$$\mathbf{K} = \begin{bmatrix} 12EI/l^3 & 6EI/l^2 & -12EI/l^3 & 6EI/l^2 & & \\ 6EI/l^2 & 4EI/l & -6EI/l^2 & 2EI/l & & \\ -12EI/l^3 & -6EI/l^2 & 12EI/l^3 + k_p & -6EI/l^2 & -k_p & \\ 6EI/l^2 & 2EI/l & -6EI/l^2 & 4EI/l & & \\ & & -k_p & & k_p + k_b & -k_b \\ & & & & -k_b & k_b + k_f \end{bmatrix}$$

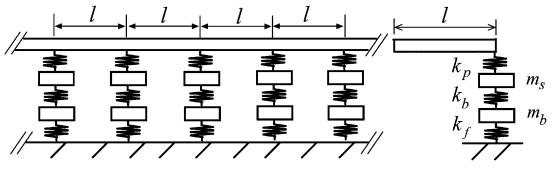


Fig. 3. The periodic track model and the repeating structure used to analyze it.

$$\mathbf{M}=\begin{bmatrix}\mathbf{M}_u & \mathbf{0}\\ \mathbf{0} & \mathbf{M}_d\end{bmatrix},\quad \mathbf{M}_u=\frac{m_r}{420}\begin{bmatrix}156 & 22l & 54 & -13l\\ 22l & 4l^2 & 13l & -3l^2\\ 54 & 13l & 156 & -22l\\ -13l & -3l^2 & -22l & 4l^2\end{bmatrix},\quad \mathbf{M}_d=\begin{bmatrix}m_s & 0\\ 0 & m_b\end{bmatrix}$$

Hence Section 4.1 gives $\mathbf{K}^*_{aa}$, $\mathbf{K}^*_{ab}$, $\mathbf{K}^*_{ba}$ and $\mathbf{K}^*_{bb}$ and these are used in Eq. (19).

## 5. Solution of the coupled vehicle–track system

In this section, the equation of motion of the coupled system excited by the harmonic track irregularity $\tilde{\mathbf{R}}(t)$ is set up and any required response PSD can also be derived.

### 5.1. Equation of motion of the vehicle

The equation of motion of the vehicle is [1]

$$(\mathbf{K}_v+\mathrm{i}\omega\mathbf{C}_v-\omega^2\mathbf{M}_v)\mathbf{u}_v=\mathbf{K}_v^d\mathbf{u}_v=\mathbf{f}_v \tag{17}$$

where $\mathbf{M}_v$, $\mathbf{C}_v$ and $\mathbf{K}_v$ are the $(10\times 10)$ mass, damping and stiffness matrices of the vehicle, respectively, $\mathbf{K}_v{}^d$ is the dynamic stiffness matrix; $\mathbf{u}_v$ is the displacement vector and; $\mathbf{f}_v$ is the force vector.

$$\mathbf{u}_v=\{u_c,\theta_c,u_{t1},\theta_{t1},u_{t2},\theta_{c2},u_{w1},u_{w2},u_{w3},u_{w4}\}^{\mathrm{T}} \tag{18a}$$

$$\mathbf{f}_v=\{0,0,0,0,0,0,f_1,f_2,f_3,f_4\}^{\mathrm{T}} \tag{18b}$$

here $f_i$ $(i=1,\,2,\,3,\,4)$ is the wheel–rail force.

### 5.2. The equation of motion of the track substructures subjected to wheel–rail forces

As shown in Fig. 1, because in practice $2l_t$ and $2(l_c-l_t)$ both exceed the sleeper spacing $l$ there are four substructures subjected to wheel–rail forces. According to Eq. (14), the equation of motion of the $i$th substructure is

$$\begin{bmatrix}\mathbf{K}^*_{aa} & \mathbf{K}^*_{ab}\\ \mathbf{K}^*_{ba} & \mathbf{K}^*_{bb}\end{bmatrix}\begin{Bmatrix}\mathbf{b}_i\\ \mathbf{a}_i\end{Bmatrix}=\mathbf{K}_t^d\begin{Bmatrix}\mathbf{b}_i\\ \mathbf{a}_i\end{Bmatrix}=-\mathbf{N}(\xi_i)f_i\quad(i=1,2,3,4) \tag{19}$$

where $\boldsymbol{K}_t^d$ is the dynamic stiffness matrix of the substructure, $\xi_i$ is the distance from the left-hand interface of the $i$th substructure to the location of $f_i$, $\mathbf{N}(\xi)$ is the shape function column vector of the Bernoulli–Euler beam element, and $\mathbf{a}_i$, $\mathbf{b}_i$ are vectors containing the two unknowns. From Eq. (15), the displacement vectors at the left- and right-hand interfaces of the $j$th substructure, $\mathbf{u}_{l,ij}$ and $\mathbf{u}_{r,ij}$, caused by $f_i$ can be expressed as

$$\mathbf{u}_{l,ij}=\mathbf{X}_a\boldsymbol{\mu}^{k-1}\mathbf{a}_i,\quad \mathbf{u}_{r,ij}=\mathbf{X}_a\boldsymbol{\mu}^{k}\mathbf{a}_i,\quad k\geqslant 1 \tag{20a}$$

$$\mathbf{u}_{l,ij}=\mathbf{X}_b\boldsymbol{\mu}^{-k}\mathbf{b}_i,\quad \mathbf{u}_{r,ij}=\mathbf{X}_b\boldsymbol{\mu}^{-k-1}\mathbf{b}_i,\quad k\leqslant -1 \tag{20b}$$

where $k$ represents the number of interfaces between the center of the $j$th substructure and the $i$th interaction force. Finally, a $(4\times4)$ matrix $\mathbf{w}^{ij}$, which will be used in Eq. (26), is defined as

$$\mathbf{w}^{ij}=\begin{cases}\begin{bmatrix}\mathbf{0}_2 & \mathbf{X}_a\boldsymbol{\mu}^{k-1}\\ \mathbf{0}_2 & \mathbf{X}_a\boldsymbol{\mu}^{k}\end{bmatrix} & \text{if } j>i\\ \begin{bmatrix}\mathbf{X}_b\boldsymbol{\mu}^{-k} & \mathbf{0}_2\\ \mathbf{X}_b\boldsymbol{\mu}^{-k-1} & \mathbf{0}_2\end{bmatrix} & \text{if } j<i\\ \begin{bmatrix}\mathbf{X}_b & \mathbf{0}_2\\ \mathbf{0}_2 & \mathbf{X}_a\end{bmatrix} & \text{if } i=j\end{cases} \tag{21}$$

where $\mathbf{0}_2$ represents the a $(2\times2)$ null matrix.

### 5.3. The equation of motion of the coupled system

The linear spring $k_h$ of Fig. 1 connects a wheelset to the beam, which represents a pair of rails, so that the wheel–rail force $f_i$ can be expressed as

$$f_i=k_h(u_{ti}+r_i-u_{wi}),\quad i=1,2,3,4 \tag{22}$$

where $u_{ti}$ is the displacement of the pair of rails at the $i$th contact point; $u_{wi}$ the displacement of the $i$th wheelset and $r_i$ the pseudo track irregularity, see Eq. (9). Because the coupled system is linear, the left- and right-hand displacement vectors of the $i$th substructure, $u_{l,i}$ and $u_{r,i}$, can be obtained as the sum of the responses caused by each of the four wheel–rail forces, i.e.

$$\mathbf{u}_{l,i}=\sum_{j=1}^{4}\mathbf{u}_{l,ji},\quad \mathbf{u}_{r,i}=\sum_{j=1}^{4}\mathbf{u}_{r,ji} \tag{23}$$

Hence, $u_{ti}$ can be obtained from the $\mathbf{N}(\xi_i)^{\mathrm{T}}$ of Eq. (19) as

$$u_{ti}=\mathbf{N}(\xi_i)^{\mathrm{T}}\begin{Bmatrix}\mathbf{u}_{l,i}\\ \mathbf{u}_{r,i}\end{Bmatrix} \tag{24}$$

Substituting Eqs. (20)–(24) into Eqs. (17) and (19) and writing them as a single equation gives the equation of motion of the coupled system as

$$\overline{\mathbf{K}}\,\overline{\mathbf{U}}=\overline{\mathbf{F}} \tag{25}$$

$$\overline{\mathbf{K}}=\begin{bmatrix}\overline{\mathbf{K}}_{vv} & \overline{\mathbf{K}}_{vt}\\ \overline{\mathbf{K}}_{tv} & \overline{\mathbf{K}}_{tt}\end{bmatrix} \tag{26}$$

$$\overline{\mathbf{K}}_{vv}=\mathbf{K}_v^d+\mathrm{diag}[0,0,0,0,0,0,k_h,k_h,k_h,k_h]$$

$$\bar{\mathbf{K}}_{tt}=\begin{bmatrix}\mathbf{k}_{tt}^{11} & \mathbf{k}_{tt}^{12} & \mathbf{k}_{tt}^{13} & \mathbf{k}_{tt}^{14}\\ \mathbf{k}_{tt}^{21} & \mathbf{k}_{tt}^{22} & \mathbf{k}_{tt}^{23} & \mathbf{k}_{tt}^{24}\\ \mathbf{k}_{tt}^{31} & \mathbf{k}_{tt}^{32} & \mathbf{k}_{tt}^{33} & \mathbf{k}_{tt}^{34}\\ \mathbf{k}_{tt}^{41} & \mathbf{k}_{tt}^{42} & \mathbf{k}_{tt}^{43} & \mathbf{k}_{tt}^{44}\end{bmatrix},\quad \mathbf{k}_{tt}^{ij}=\begin{cases}k_h\mathbf{N}(\xi_i)\mathbf{N}(\xi_i)^{\mathrm{T}}w^{ij} & \text{if } i\neq j\\ \mathbf{K}_t^d+k_h\mathbf{N}(\xi_i)\mathbf{N}(\xi_i)^{\mathrm{T}}w^{ij} & \text{if } i=j\end{cases}$$

$$\overline{\mathbf{K}}_{vt}=\begin{bmatrix}\mathbf{0}_{6\times4} & \mathbf{0}_{6\times4} & \mathbf{0}_{6\times4} & \mathbf{0}_{6\times4}\\ \mathbf{K}_{vt}^1 & \mathbf{K}_{vt}^2 & \mathbf{K}_{vt}^3 & \mathbf{K}_{vt}^4\end{bmatrix},\quad \mathbf{K}_{vt}^j=[\mathbf{k}_{vt}^{1j},\ \mathbf{k}_{vt}^{2j},\ \mathbf{k}_{vt}^{3j},\ \mathbf{k}_{vt}^{4j}]^{\mathrm{T}},\quad \mathbf{k}_{vt}^{ij}=-k_h\mathbf{N}(\xi_i)^{\mathrm{T}}\mathbf{w}^{ij}$$

$$\overline{\mathbf{K}}_{tv}=\begin{bmatrix}\mathbf{0}_{4\times6} & \mathbf{K}_{tv}^1\\ \mathbf{0}_{4\times6} & \mathbf{K}_{tv}^2\\ \mathbf{0}_{4\times6} & \mathbf{K}_{tv}^3\\ \mathbf{0}_{4\times6} & \mathbf{K}_{tv}^4\end{bmatrix},\quad \begin{aligned}\mathbf{K}_{tv}^1&=[-k_h\mathbf{N}(\xi_1),\mathbf{0}_{4\times1},\mathbf{0}_{4\times1},\mathbf{0}_{4\times1}]\\ \mathbf{K}_{tv}^2&=[\mathbf{0}_{4\times1},-k_h\mathbf{N}(\xi_2),\mathbf{0}_{4\times1},\mathbf{0}_{4\times1}]\\ \mathbf{K}_{tv}^3&=[\mathbf{0}_{4\times1},\mathbf{0}_{4\times1},-k_h\mathbf{N}(\xi_3),\mathbf{0}_{4\times1}]\\ \mathbf{K}_{tv}^4&=[\mathbf{0}_{4\times1},\mathbf{0}_{4\times1},\mathbf{0}_{4\times1},-k_h\mathbf{N}(\xi_4)]\end{aligned}$$

$$\mathbf{U}=\{\mathbf{u}_v,\mathbf{b}_1,\mathbf{a}_1,\mathbf{b}_2,\mathbf{a}_2,\mathbf{b}_3,\mathbf{a}_3,\mathbf{b}_4,\mathbf{a}_4\}^{\mathrm{T}} \tag{27}$$

$$\begin{aligned}\mathbf{F}_{vt}=k_h\{&0,0,0,0,0,0,\mathrm{e}^{-\mathrm{i}\omega t_1},\mathrm{e}^{-\mathrm{i}\omega t_2},\mathrm{e}^{-\mathrm{i}\omega t_3},\mathrm{e}^{-\mathrm{i}\omega t_4},\\ &-\mathbf{N}(\xi_1)^{\mathrm{T}}\mathrm{e}^{-\mathrm{i}\omega t_1},-\mathbf{N}(\xi_2)^{\mathrm{T}}\mathrm{e}^{-\mathrm{i}\omega t_2},-\mathbf{N}(\xi_3)^{\mathrm{T}}\mathrm{e}^{-\mathrm{i}\omega t_3},\mathbf{N}(\xi_4)^{\mathrm{T}}\mathrm{e}^{-\mathrm{i}\omega t_4}\}^{\mathrm{T}}\sqrt{\tilde{S}_r(\omega)}\,\mathrm{e}^{\mathrm{i}\omega t}\end{aligned} \tag{28}$$

where $\mathbf{0}_{m\times n}$ denotes an $(m\times n)$ null matrix. The coupled system consists of a vehicle and four track substructures, so that $\overline{\mathbf{K}}$ is the $26\times26$ dynamic stiffness matrix of the coupled system; $\overline{\mathbf{U}}$ is the response vector and; $\overline{\mathbf{F}}$ is the pseudo force vector. Any pseudo response of the coupled system, $\tilde{u}$, can be obtained by solving Eq. (25), then using PEM to obtain the response PSD from

$$S(\omega)=\tilde{u}\tilde{u}^* \tag{29}$$

where the superscript denotes complex conjugate.

## 6. Numerical examples

The vehicle and track parameters used in the example are listed in Tables 1 and 2, and [1] the American track spectrum function for line grade 6 is adopted when $\Omega\leqslant2\pi$ and otherwise the function proposed by the Chinese Railway Science Academy is used, giving

$$\begin{aligned}S_r(\Omega)&=\frac{kA_v\Omega_c^2}{\Omega^2(\Omega^2+\Omega_c^2)}(\mathrm{cm}^2/\mathrm{rad/m}) \qquad (\Omega\leqslant2\pi)\\ k&=0.25,\ \ A_v=0.0339,\ \ \Omega_c=0.8245\\ S_r(\Omega)&=0.036(\Omega/2\pi)^{-3.15}(\mathrm{mm}^2/\mathrm{rad/m}) \quad (\Omega>2\pi)\end{aligned} \tag{30}$$

In order to demonstrate the track frequency-response characteristics for this example, the absolute values, $|\mu_1|$ and $|\mu_2|$, of the first two wave propagation coefficients are shown versus frequency in Fig. 4. It can be seen that in the frequency ranges 0–45 and 65–100 Hz these two absolute values are almost identical and are both

Table 1
Vehicle parameters

| | | | |
|---|---|---|---|
| Vehicle body mass $M_c$ | $34\times10^3$ kg | Secondary suspension stiffness of vehicle $k_c$ | $800\times10^3$ N/m |
| Bogie mass $M_t$ | 3000 kg | Secondary suspension damping of vehicle $c_c$ | $160\times10^3$ N s/m |
| Wheelset mass $M_w$ | 1400 kg | Primary suspension stiffness of vehicle $k_t$ | $1100\times10^3$ N/m |
| Vehicle body moment of inertia $J_c$ | $2.277\times10^6$ m$^4$ | Primary suspension damping of vehicle $c$ | $12\times10^3$ N s |
| Bogie moment of inertia $J_t$ | 2710 m$^4$ | Half of bogie spacing, $=l_c$ | 9 m |
| Wheel–rail contact constant $G$ | $5.135\times10^{-8}$ m/N$^{2/3}$ | Half of wheelset spacing, $=l_t$ | 1.2 m |

Table 2
Track parameters

| | | | |
|---|---|---|---|
| Mass of rail $m_r$ | 121.28 kg/m | Railpad stiffness $k_p$ | $15.6\times10^7$ N/m |
| Rail bending stiffness $EI$ | $13.25\times10^6$ N m$^2$ | Ballast stiffness $k_b$ | $4.8\times10^8$ N/m |
| Sleeper mass $m_s$ | 237 kg | Subgrade stiffness $k_f$ | $13\times10^7$ N/m |
| Ballast mass $m_b$ | 1365.2 kg | Sleeper spacing $l$ | 0.54 m |

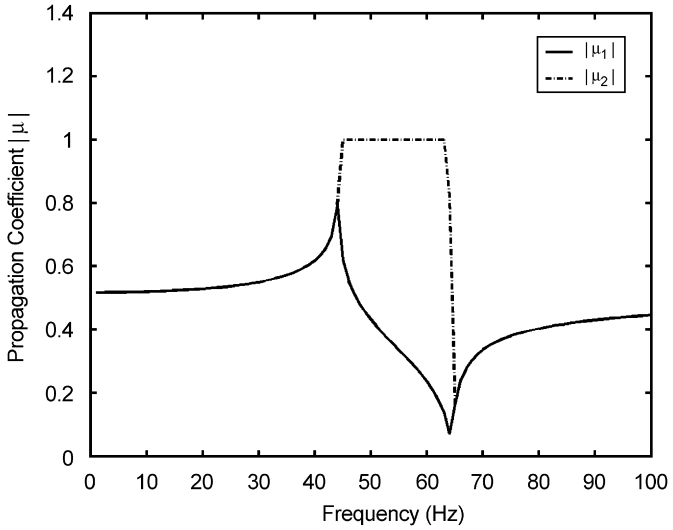


Fig. 4. Wave propagation coefficients.

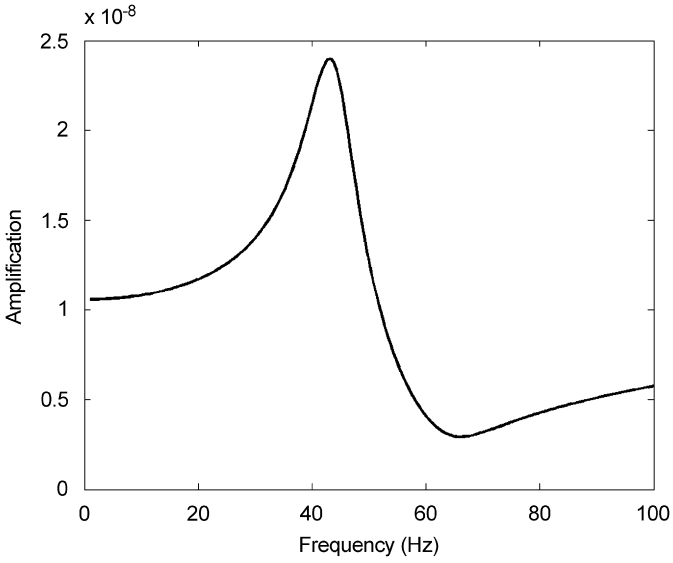


Fig. 5. Harmonic response amplification.

less than 1, so that the corresponding waves will decrease when propagating, whereas in the frequency range 45–65 Hz they are quite different, such that $|\mu_1|$ is always significantly less than 1 whereas $|\mu_2|$ is equal to 1 for much of the range to which the corresponding wave will remain its amplification during propagation. Note that the damping is not included in Fig. 4. If considering the damping, $|\mu_1|$ and $|\mu_2|$ will be always less than 1. Fig. 5 shows the vibration amplification of the rails at the middle of a substructure, which has unit harmonic force applied there, and it can be seen that the track resonates when the frequency is a little above 40 Hz. Here, the damping coefficient is 0.2.

In order to test the correctness of the method and program of this paper its results for the vehicle body and bogie accelerations and for the wheel–rail force PSDs are compared in Fig. 6, for $V = 100$ km/h and the track damping coefficient is $v = 0.2$, with FEM results for which the beam which represents the rails is modelled as having finite length and clamped ends, with the length chosen such that each end of the beam is 20 m from the

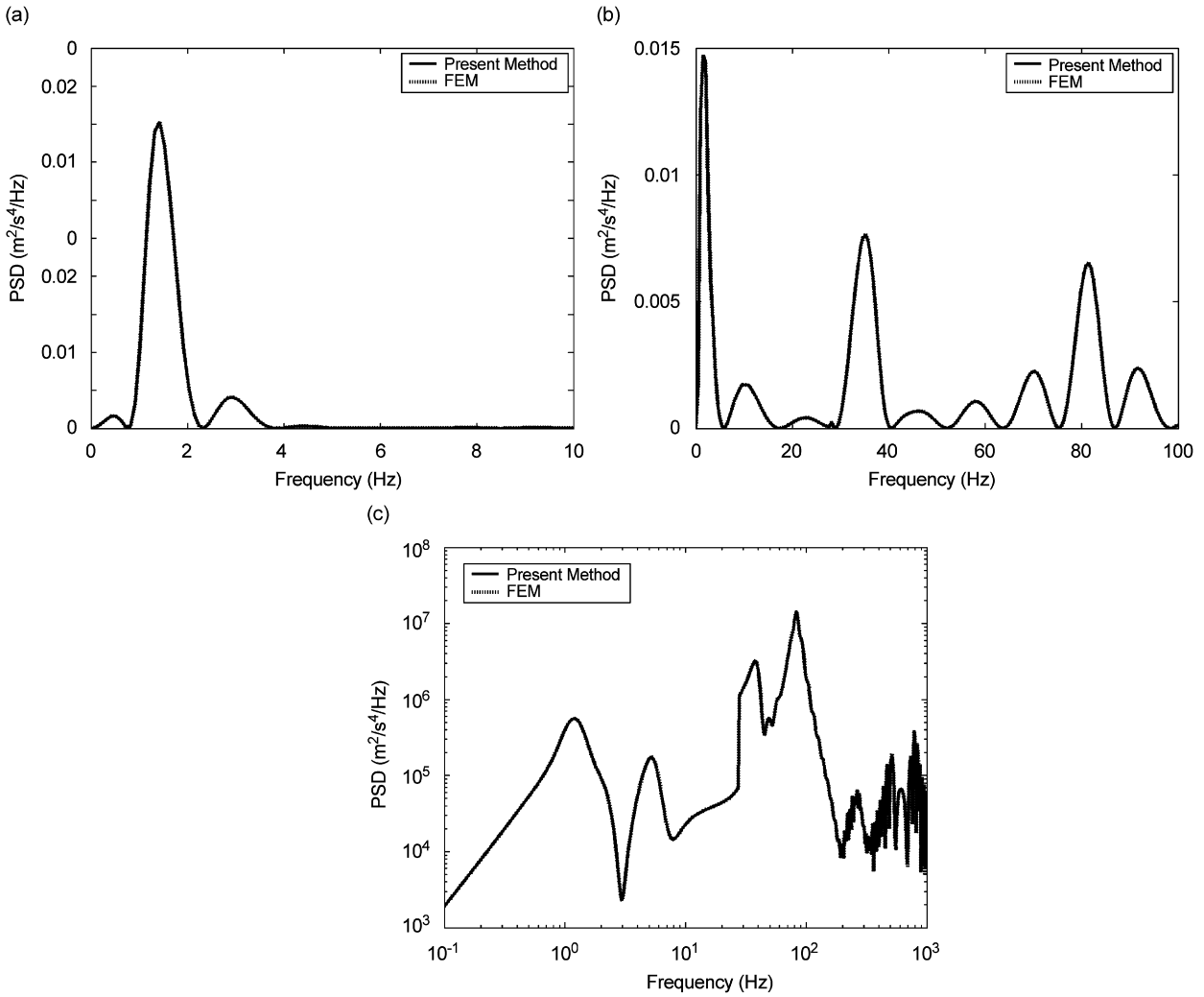


Fig. 6. Comparison between results given by the present method and those given by FEM: (a) vertical acceleration PSD of vehicle body; (b) vertical acceleration PSD of bogie 1; (c) wheel–rail force PSD of wheelset 1.

nearest wheelset. As is usual in practice, in these results the wheel–rail forces presented are for contact between one wheel and one rail. It can be seen that the results given by the two methods agree well although there are small differences due to the clamped boundary conditions assumed by the FEM analysis. The present method and FEM gave identical standard deviations for the three responses: 0.1125 m/s$^2$, 0.4010 m/s$^2$ and 18.76 kN, respectively. Hence, the appropriateness of the method and program are verified. Moreover, the PSD for the vehicle body has by far its largest values in the vicinity of 1.5 Hz, i.e. close to the fundamental frequency of the vehicle, whereas the PSD for the bogie has peaks there and also at about 40 and 80 Hz. Obviously, the peak near 1.5 Hz is caused by the vehicle body and the peaks at 40 and 80 Hz are caused by wheel–rail forces. These are shown in Fig. 6(c) which also shown peaks around 1.5, 40 and 80 Hz, but which has several more peaks in the frequency range 200–1000 Hz. Similar conclusions were drawn in Ref. [1].

The traditional model assumes that the vehicle moves on rigid rails which rest on a rigid foundation but which have the profile $r(x)$. Fig. 7 compares the vehicle body acceleration and wheel–rail force PSDs given by this traditional model with those given by the model of this paper, for $V = 160$ km/h and $v = 0.2$. Clearly, there is excellent agreement in the low-frequency region, but in the high-frequency region there are major differences. The wheel–rail force PSD for the traditional model has a resonance peak near 200 Hz, i.e. close to

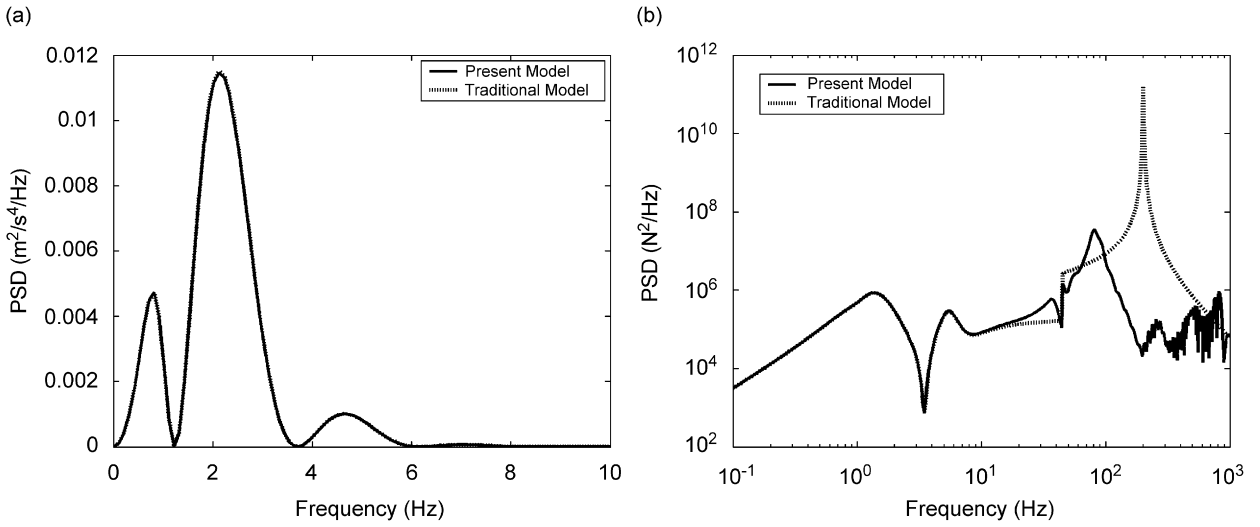


Fig. 7. Comparison between results given by the present model and those given by the traditional model: (a) vertical acceleration PSD of vehicle body; (b) wheel–rail force PSD.

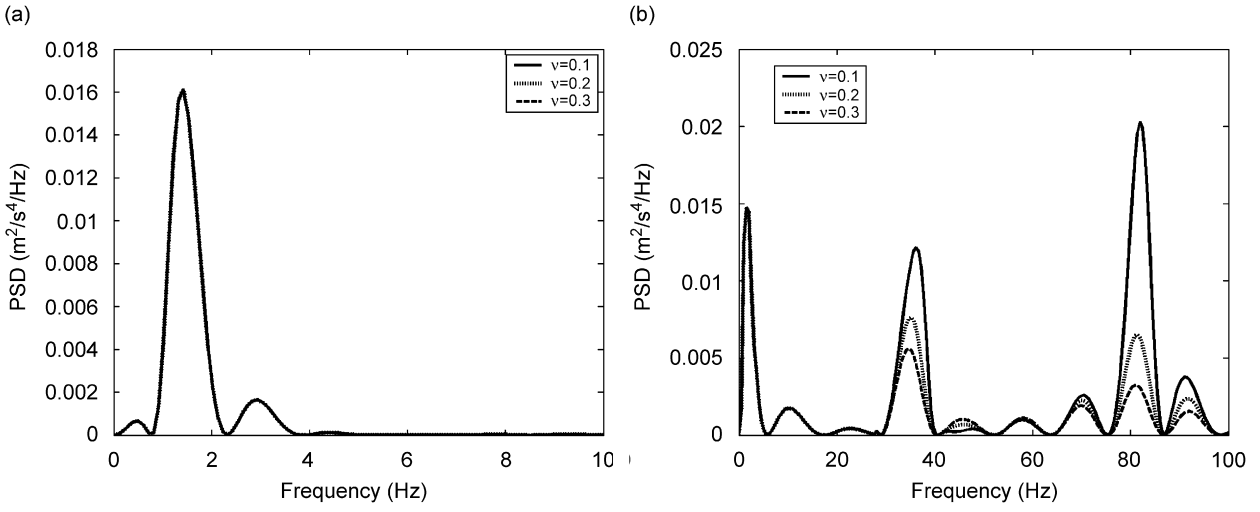


Fig. 8. Influence of track damping: (a) vertical acceleration PSD of vehicle body; (b) vertical acceleration PSD of the bogie.

the free vibration frequency of the wheelset, $\sqrt{k_h/M_w}/2\pi \simeq 201$ Hz, whereas the PSD for the present model has a peak at about 80 Hz which is caused by the interaction of wheelset and rails. Therefore, because the vehicle body response is mainly in the low frequency range it is reasonable to use the traditional model to analyze it.

Damping is a very important characteristic for structures. Therefore, hysteretic damping is taken into account, using the method given in the paragraph beneath Eq. (15). Fig. 8 shows the vehicle body and the bogie acceleration PSDs for track damping coefficients of $v = 0.1$, 0.2 and 0.3 when $V = 100$ km/h. It can be seen that damping influences the vehicle body responses insignificantly because they occur mainly in the low frequency range, whereas increasing it may significantly reduce the bogie acceleration PSD in the high-frequency region.

Vehicle velocity also has an important influence on the responses, as Fig. 9 shows. However, it can be seen that increasing the velocity does not always give stronger responses. Thus, for $V = 120$ km/h the peak of

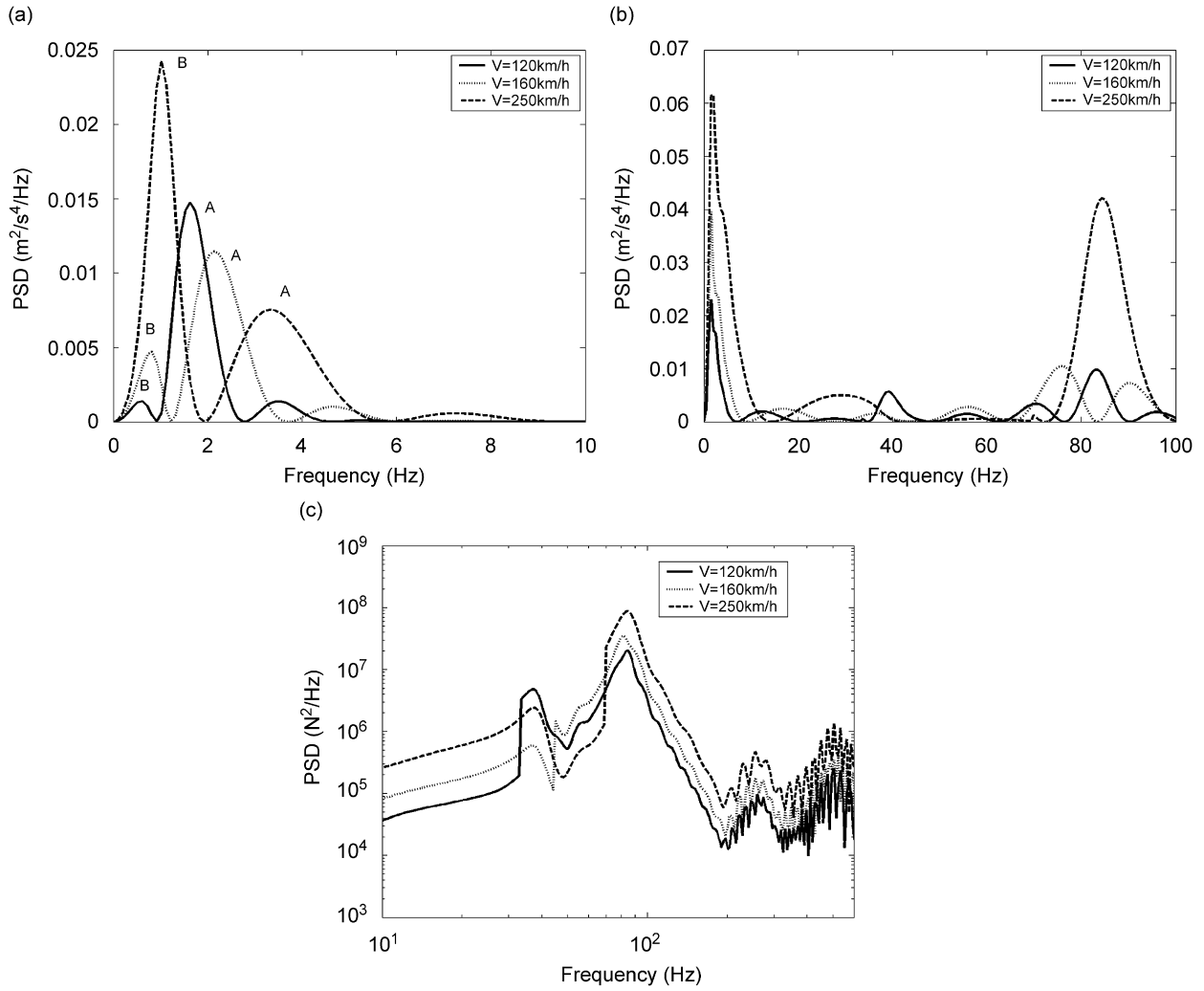


Fig. 9. Influence of vehicle velocity, for $v = 0.2$: (a) vehicle body response; (b) bogie response; (c) wheel–rail force.

vehicle body vertical acceleration PSD is at about 1.8 Hz, decreases and shifts up to about 2 Hz at $V = 160$ km/h and then increases greatly and shifts back to around 1 Hz at $V = 250$ km/h. To explain this, results were obtained for $V = 80, 90, \ldots, 240, 250$ km/h and these showed that the peaks denoted by A and B on Fig. 9(a) both moved to the right as $V$ increased, but that the peak at A was decreasing while that at B was increasing, such that they were of equal height at approximately $V = 190$ km/h. Generally speaking, the response peaks may appear at the resonant frequencies due to the frequency-response function, but not always distinctly so. The distribution of the excitation PSD in the frequency domain may very strongly influence the response. Moreover, for multiexcitation problems, the influence of different excitations on an arbitrary response may be superposed or may counteract each other. For the vehicle–track system discussed, the vehicle velocity decides the time lags between the wheel–rail contact forces as well as the distribution of external excitations in the frequency domain caused by the track irregularity. Each of them may play a dominant role for the distribution of the response PSD in the frequency domain. For the bogie vertical acceleration PSD, the peak value in the high-frequency region at velocity 120 km/h is almost equal to that at 160 km/h. The reason is that the influences of the wheel–rail forces acting on the bogie and hence on the vehicle body cancel each other due to time lags at velocity 160 km/h. For wheel–rail forces, the peak value increases with increasing velocity.

## 7. Conclusions

PEM and symplectic solution methodology have been combined to study random vibration of vehicle–track coupled systems. PEM is used to transform the random multiexcitation problem into a deterministic harmonic excitation one and a symplectic solution method has been applied to account for the track harmonic responses. The numerical example has verified the accuracy of the proposed method and program; compared results from the present model with those from the traditional rigid track model and; been used to investigate the influences of track damping and vehicle velocity. The following conclusions can be drawn:

1. The traditional model is suitable for analyzing vehicle body response, but for bogie response and for wheel–rail interaction forces the coupled system is more reliable.
2. Damping of the track has negligible effect on vehicle body response but influences bogie response PSDs and wheel–rail interaction force PSDs significantly.
3. Vehicle velocity influences the response PSDs significantly, but they do not increase monotonically with velocity.

## Acknowledgments

The authors are grateful for support from the National Natural Science Foundation of China (Grant nos. 10472023 and 10502011); the doctoral research fund of the Chinese Ministry of Education (Grant no. 20040141020) and the Cardiff Advanced Chinese Engineering Centre.

## References

[1] G. Chen, Analysis of Random Vibration for Vehicle and Track Coupling System, PhD Thesis, South West Jiaotong University, 2000 (Chapter 3) (in Chinese).
[2] G. Chen, Analysis of Random Vibration for Vehicle and Track Coupling System, PhD Thesis, South West Jiaotong University, 2000 (Chapter 5) (in Chinese).
[3] X. Lei, N.A. Noda, Analyses of dynamic response of vehicle and track coupling system with random irregularity of track vertical profile, *Journal of Sound and Vibration* 258 (2002) 147–165.
[4] W.M. Zhai, *Vehicle– Track Coupling Dynamics Railway*, Chinese Railway Press, Beijing, 2002 (in Chinese).
[5] L. Gry, Dynamic modelling of railway track based on wave propagation, *Journal of Sound and Vibration* 195 (1996) 477–505.
[6] L. Gry, C. Gontier, Dynamic modelling of railway track: a periodic model based on a generalized beam formulation, *Journal of Sound and Vibration* 199 (1997) 531–558.
[7] D.J. Thompson, Vehicle–rail noise generation—part 3: rail vibration, *Journal of Sound and Vibration* 161 (1993) 421–446.
[8] H. Kruse, K. Popp, T. Krzyzynski, On steady state dynamics of railway tracks modeled as continuous periodic structures, *Machine Dynamics Problems* 20 (1998) 149–166.
[9] F.W. Williams, W.X. Zhong, P.N. Bennett, Computation of the eigenvalues of wave propagation in periodic sub-structural systems, *Journal of Vibration and Acoustics* 115 (1993) 422–426.
[10] W.X. Zhong, F.W. Williams, Wave problems for repetitive structures and symplectic mathematics, *Proceedings of the Institution of Mechanical Engineers, Part C* 206 (1992) 371–379.
[11] W.X. Zhong, J.H. Lin, C.H. Qiu, Eigenproblem of sub-structural chain and the expansion solution, *Acta Mechanica Sinica* 7 (1991) 169–177.
[12] W.X. Zhong, F.W. Williams, The eigensolutions of wave propagation for repetitive structures, *International Journal of Structural Engineering and Mechanics* 1 (1993) 47–60.
[13] J.H. Lin, Y. Fan, P.N. Bennett, F.W. Williams, Propagation of stationary random waves along substructural chains, *Journal of Sound and Vibration* 180 (1995) 757–767.
[14] J.H. Lin, Y. Fan, F.W. Williams, Propagation of non-stationary waves along substructural chains, *Journal of Sound and Vibration* 187 (1995) 585–593.
[15] F.W. Williams, P.N. Bennett, J.H. Lin, Localization investigation of stationary random wave transmission along damped ordered structural chains, *Proceedings of the Institution of Mechanical Engineers, Part C* 21 (1997) 217–228.
[16] J.H. Lin, J.J. Li, W.S. Zhang, F.W. Williams, Non-stationary random seismic responses of multi-support structures in evolutionary inhomogeneous random fields, *Earthquake Engineering and Structural Dynamics* 26 (1997) 135–145.
[17] J.H. Lin, Y.H. Zhang, *Vibration and Shock Handbook, Seismic Random Vibration of Long-span Structures*, CRC Press, Boca Raton, FL, 2005 (Chapter 30).
[18] J.H. Lin, W.S. Zhang, J.J. Li, Structural responses to arbitrarily coherent stationary random excitations, *Computers and Structures* 50 (1994) 629–633.